

## Neon seeded ITER baseline scenario experiments in JET D and D-T plasmas

I.S. Carvalho<sup>1</sup>, C. Giroud<sup>2</sup>, D.B. King<sup>2</sup>, D. L. Keeling<sup>2</sup>, L. Frassinetti<sup>3</sup>, R. A. Pitts<sup>1</sup>, S. Wiesen<sup>4</sup>, G. Pucella<sup>5</sup>, A. Kappatou<sup>6</sup>, N. Vianello<sup>7</sup>, M. Wischmeier<sup>6</sup>, F. Rimini<sup>2</sup>, M. Baruzzo<sup>5</sup>, M. Maslov<sup>2</sup>, M. Sos<sup>8</sup>, X. Litaudon<sup>9</sup>, R. B. Henriques<sup>2</sup>, K. Kirov<sup>2</sup>, C. Perez von Thun<sup>10</sup>, H. J. Sun<sup>2</sup>, M. Lennholm<sup>2</sup>, J. Mitchell<sup>2</sup>, A. Parrot<sup>2</sup>, J. Bernardo<sup>2</sup>, M. Zerbini<sup>5</sup>, I. Coffey<sup>11</sup>, K. Collie<sup>2</sup>, J.M. Fontdecaba<sup>12</sup>, N. Hawkes<sup>2</sup>, Z. Huang<sup>2</sup>, I. Jecu<sup>2</sup>, D. Kos<sup>2</sup>, K. Lawson<sup>2</sup>, E. Litherland-Smith<sup>2</sup>, A. Meigs<sup>2</sup>, C. Olde<sup>2</sup>, A. Patel<sup>2</sup>, L. Piron<sup>7</sup>, M. P. Poradzinski<sup>2,10</sup>, Z. Stancar<sup>2</sup>, D. Taylor<sup>2</sup>, E. Alessi<sup>13</sup>, I. Balboa<sup>2</sup>, A. Boboc<sup>2</sup>, S. Bakes<sup>2</sup>, M. Brix<sup>2</sup>, E. De la Cal<sup>12</sup>, P. Carvalho<sup>2</sup>, A. Chomiczewska<sup>10</sup>, Z. Ghani<sup>2</sup>, E. Giovannozzi<sup>5</sup>, J. Foster<sup>2</sup>, A. Huber<sup>14</sup>, J. Karhunen<sup>15</sup>, E. Kowalska-Strzeciwilk<sup>10</sup>, J. Maddock<sup>2</sup>, J. Matthews<sup>2</sup>, S. Menmuir<sup>2</sup>, K. Mikszuta<sup>10</sup>, R. B. Morales-Bianchetti<sup>2</sup>, E. Pawelec<sup>16</sup>, G. Petravich<sup>16</sup>, E. Pinto<sup>12</sup>, I. Voldiner<sup>12</sup>, G. Sergienko<sup>14</sup>, S. Silburn<sup>2</sup>, J. Svodoba<sup>8</sup>, M. Tomes<sup>8</sup>, B. Thomas<sup>2</sup>, A. Tookey<sup>2</sup>, Y. Zayachuk<sup>2</sup>, M. Valovic<sup>2</sup>, A. Widdowson<sup>2</sup>, L. Xiang<sup>2</sup>, F. Auremma<sup>7</sup>, P. Innocente<sup>7</sup>, S. Gabriellini<sup>17</sup>, A. Mariani<sup>13</sup>, M. Marin<sup>18</sup>, I. Predebon<sup>7</sup>, A. Thysoe<sup>19</sup>, V.K. Zotta<sup>17</sup>, JET Contributors\* and the EUROfusion Tokamak Exploitation Team\*\*

<sup>1</sup>ITER Organization, Route de Vinon-sur-Verdon, CS 90 046, 13067 St Paul Lez Durance Cedex, France; <sup>2</sup>United Kingdom Atomic Energy Authority, Culham Campus, Abingdon OX14 3DB, UK; <sup>3</sup>Division of Electromagnetic Engineering and Fusion Science, KTH Royal Institute of Technology, Stockholm SE; <sup>4</sup>DIFFER - Dutch Institute for Fundamental Energy Research, De Zaale 20, 5612 AJ Eindhoven, Netherlands; <sup>5</sup>Fusion and Nuclear Safety Department - ENEA C. R. Frascati - via E. Fermi 45, 00044 Frascati (Roma), Italy; <sup>6</sup>Max-Planck-Institut für Plasmaphysik, Garching, Germany; <sup>7</sup>Consorzio RFX, Corso Stati Uniti, 4, Padova, 35127 Italy; <sup>8</sup>Institute of Plasma Physics of the CAS, Za Slovankou 1782/3, 182 00 Prague 8, Czech Republic; <sup>9</sup>CEA, IRFM, F-13108 Saint Paul Lez Durance, France; <sup>10</sup>Institute of Plasma Physics and Laser Microfusion, Hery 23, 01-497 Warsaw, Poland; <sup>11</sup>Astrophysics Research Centre, School of Mathematics and Physics, Queen's University, Belfast, BT7 1NN; <sup>12</sup>Laboratorio Nacional Fusión. CIEMAT. Av Complutense 40. 28040 Madrid. Spain; <sup>13</sup>Institute for Plasma Science and Technology, CNR, 20125 Milano, Italy; <sup>14</sup>Forschungszentrum Jülich GmbH, Institute of Fusion Energy and Nuclear Waste Management – Plasma Physics, Partner of the Trilateral Euregio Cluster (TEC), 52425 Jülich, Germany; <sup>15</sup>VTT Technical Research Centre of Finland, P.O. Box 1000, 02044 VTT, Finland; <sup>16</sup>Institute of Physics, University of Opole, Oleska 48, 45-052 Opole, Poland; <sup>17</sup>Sapienza University of Rome, Rome, Italy; <sup>18</sup>SPC, Swiss Plasma Center, Ecole Polytechnique Federale de Lausanne, Station 13, Lausanne 1015, Switzerland; <sup>19</sup>PPFE, DTU Physics, Technical University of Denmark, 2800 Kgs. Lyngby, Denmark; \*See the author list of "Overview of T and D-T results in JET with ITER-like wall" by CF Maggi et al. to be published in Nuclear Fusion Special Issue: Overview and Summary Papers from the 29th Fusion Energy Conference (London, UK, 16-21 October 2023); \*\*See the author list of "Progress on an exhaust solution for a reactor using EUROfusion multi-machines capabilities" by E. Joffrin et al. to be published in Nuclear Fusion Special Issue.

### 1. Introduction

The ITER baseline scenario [1] defined as the first target for ITER deuterium-tritium (DT) operation consists on an inductive scenario at 15MA, 5.3T, high triangularity ( $\delta \approx 0.45$ ),  $q_{95} \approx 3$ ,  $Q=10$  expected to be achieved with  $H_{98(y,2)}=1$ ,  $f_{GW}=0.86$ ,  $\beta_p=0.86$ , and  $v_{e,ped}^*=0.01$  for a duration greater than 300s. The integrity of the divertor requires the heat load to be maintained below  $10\text{MW}\cdot\text{m}^{-2}$ , and for this, neon impurity seeding is required to achieve a partially detached divertor state. The challenge in achieving this integrated scenario in ITER is to reduce the power load whilst maintaining sufficient impurity compression at the divertor, and midplane in order to keep the impurity content in the core plasma within an acceptable limit for the required fusion gain.

Over the past years, JET has carried out core-edge integration studies [2] dedicated to understand how the integrated scenario of ITER would work in the so-called JET ITER baseline plasmas with the following characteristics: high-triangularity ( $\delta=0.35$ -

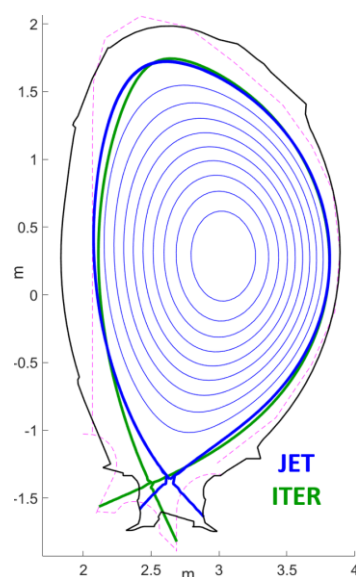


Figure 1 – Comparison between JET plasma shape (blue) and a scaled down ITER shape (green).

0.38), with divertor configuration with the inner and outer leg on the vertical targets, closer to the ITER divertor and optimal for better detachment, see figure 1. The previously best demonstration of an integrated ITER-baseline scenario with neon seeding at JET was obtained at 2.5MA/2.7T,  $H_{98(y,2)}=0.9$ ,  $\beta_N=2.2$ ,  $\delta_{av}=0.37$ ,  $f_{GW}=0.7$ ,  $f_{rad}=0.86$ ,  $Z_{eff}=2.7$ ,  $P_{NBI}=29\text{MW}$ ,  $P_{ICRH}=5\text{MW}$  with deuterium (D) gas rate of  $3.6 \times 10^{22} \text{ e.l.s}^{-1}$  and no ELMs (pulse #97490) [2][3].

Machine size and high temperature was demonstrated to be key to maintain impurities in the divertor where it is aimed for them to radiate [4][5][6]. Consequently, JET the closest tokamak in size to ITER amongst current devices is best positioned to address the core-edge integration issues. Although, we note that JET cannot reach the same neon compression, therefore, in semi-detachment state some radiation is located near the x-point (see figure 5), unlike the expectations for ITER where most radiation is expected to be below x-point [5].

The core-edge integration was one of the main topics addressed in the last JET campaigns, where the aim was to demonstrate the robustness of the 2.5MA neon seeded scenario, push the pedestal collisionality to lower values (as reasonably possible given the machine size and not to compromise the remaining scenario parameters), to port the scenario to higher current (3MA and 3.2MA) and from D to DT operation. The aim of this study not only to develop an integrated scenario for JET addressing issues faced by ITER but also to understand the key physics at play in this integration, how to achieve a high radiative divertor, its impact on the pedestal and overall confinement, as well as provide key data to improve modelling capabilities.

This paper presents only the key highlights of the last JET campaign on this topic.

## 2. High performance semi-detached Ne-seeded pulses

We have demonstrated for the first-time at high current with a high-performance neon seeded H-mode, partially detached divertor in approximately 50:50 deuterium-tritium with the following plasma parameters;  $I_p \approx 3 \text{ MA}$ ,  $W_p \approx 8 \text{ MJ}$ ,  $\beta_N \approx 2$ ,  $\delta_{av} \approx 0.35$ ,  $f_{GW} \approx 0.65$ ,  $f_{rad} \approx 0.8$ ,  $H_{98(y,2)} \approx 0.85$ ,  $T_{e,ped} \approx 1 \text{ keV}$ ,  $T_{i,ped} \approx 1.5 \times T_{e,ped}$ ,  $n_{e,ped} \approx 4.7 \times 10^{19} \text{ m}^{-3}$ ,  $q_{95} \approx 2.7$ ,  $C_{Ne} \approx 2\%$ ,  $P_{in} \approx 35 \text{ MW}$  and  $P_{fus} \approx 4\text{MW}$ . This DT plasma showed no signs of tungsten accumulation ( $C_w \approx 4 \times 10^{-6}$ ) and was held stationary for more than 6.5s with respect to the main plasma parameters including radiation, see figure 2 (pulse #104600 video available at [7]). The IR tile temperature time trace is indicative of partial detachment. The diagram on figure 3 compares the key plasma parameters obtained with the ITER values and illustrates nicely the integrated scenario with even pedestal collisionality approaching those of ITER. It is acknowledged that such a highly fuelled scenario on JET cannot reach the value of collisionality values similar to ITER, even low collisionality JET scenarios such as the JET D-T hybrid scenario

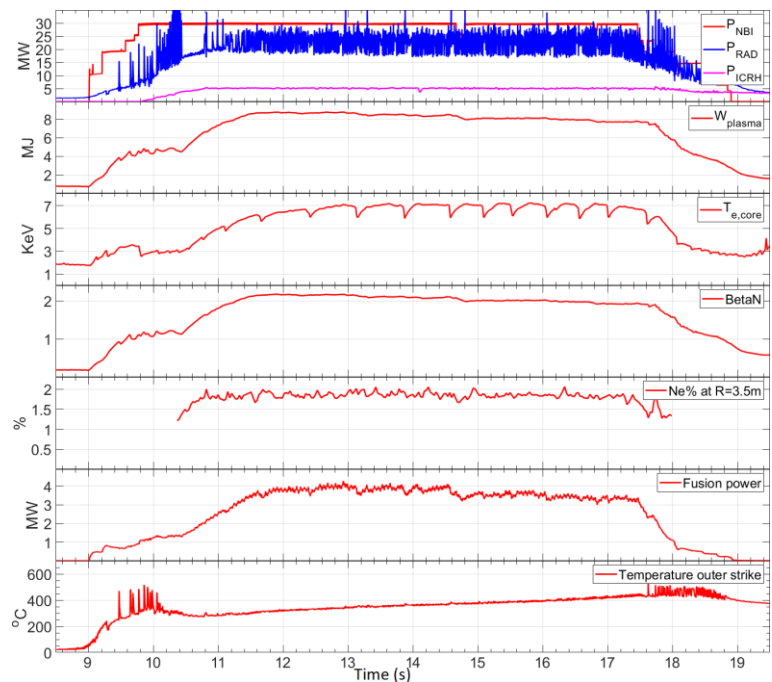


Figure 2 – #104600 High performance semi-detached D-T pulse at JET.

[8] cannot reach the expected ITER collisionality.

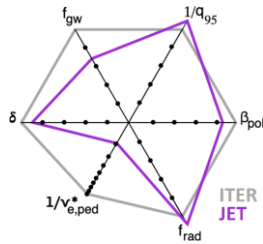


Figure 3 – Radar plot with ITER baseline parameters (grey) and parameters of JET pulse 104600 (blue)

Other similarly good demonstrations of an integrated scenario (not shown in this document) were obtained at 2.5MA in DT as well. Although not detailed in this paper, the transfer from the 2.5MA integrated scenario (such as #97490) from D to D-T was reasonably straight forward following a similar optimization scheme, and similar observation was also obtained when adapting the scenario to higher plasma current. It should be highlighted that although the ITER baseline was developed at high current first in D at 3MA and 3.2MA, however the high-performance was only obtained in DT at 3MA, not in D. The operational window for improved confinement with neon seeding is wider in DT than D (maximum input power was used in both) and it is likely due to a closer proximity to the H to L transition in D. This is currently under investigation.

### 3. Effect of neon seeding on this scenario

The main objective of neon seeding is to reduce the power flux to the divertor, this effect can clearly be observed in figure 4 where the divertor remains at lower temperature in the neon seeded pulses, in fact, it was not possible to perform unseeded pulses at full power due to the inertially cooled tiles overheating under such regime.

Figure 5 details the effect of the neon seeding on the radiation profile, as expected the total radiation increases with neon, but additionally the pattern of the radiation also changes slightly, as the neon concentration increases (from left to right on the figure) the radiation starts to move further inside relative to the x-point location.

Another important aspect of the neon seeding, observed at 2.5MA and 3MA in D and DT, is the gradual reduction in the ELM size with increasing neon seeding, this is depicted in figure 6. The reduction of the ELM size is a benefit to reduce the tungsten sputtering from the target plates helping the overall plasma tungsten content of this integrated scenario to remain low. Avoiding large ELM bursts is one critical element of the ITER integrated scenario, the ELM

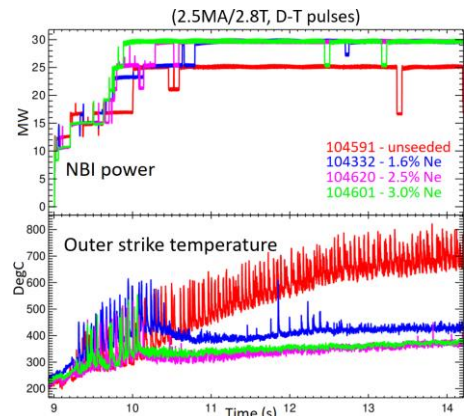


Figure 4 – outer strike point temperature (inertial cooling) for different neon seeding

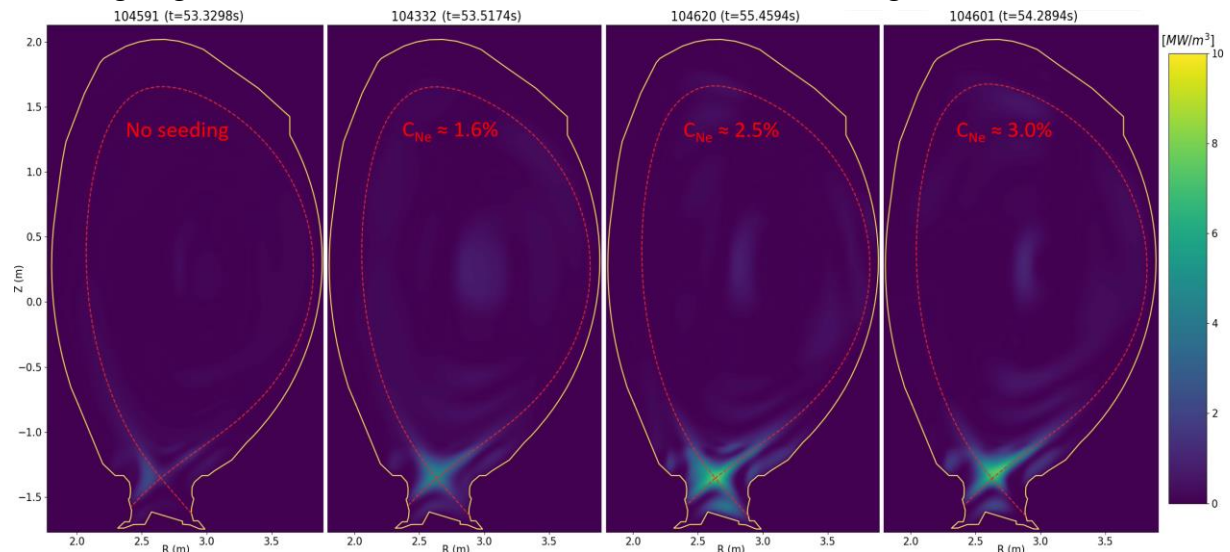


Figure 5 – Different bolometer tomographic reconstruction with increasing neon seeding (up to  $C_{Ne} \approx 3\%$ )

mitigation in ITER can however be achieved by employing additional means which are not available to JET, namely by employing the internal ELM perturbation coils.

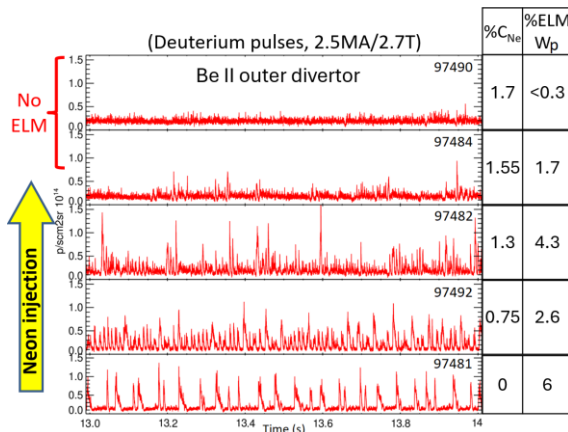


Figure 6 – From bottom to top, ELM behaviour for increasing neon seeding levels at 2.5 MA.

that the unseeded pulse cannot run at full power due to restrictions to target tile integrity (high power flux to the target due to low dissipative radiation) and that it requires an even higher fuel throughput to sustain a given ELM frequency (and lower the individual ELM size) not to accumulate excessive amounts of tungsten in the plasma which would lead to the plasma thermal collapse with time.

Assuming constant input power, if neon is pushed further, at a high enough neon concentration, the plasma performance will eventually be impacted with a too high radiative loss within the confined plasma, and if pushed even further, the H-mode will be lost.

#### 4. Conclusions and future work

An integrated scenario with stationary high-performance neon seeded baseline plasma has been obtained at JET in D-T with partially detached divertor conditions at 2.5-3MA with no ELMs and no tungsten accumulation, a particular example was a steady 3 MA, 2.9T integrated scenario with  $P_{\text{fusion}} \approx 4$  MW and a total of 27 MJ of fusion energy.

The extensive experience with this scenario allowed us to transfer the knowledge to higher currents and obtain similar results by employing a similar optimization process, proving that these results are translatable within different fuelling isotopes and different plasma currents.

JET has a wealth of data on an integrated scenario of high interest for ITER, analysis and validation of edge and core models on JET with seeded ITER baseline for more reliable prediction for ITER will be carried out for years.

#### 5. References

[1] M. Shimada *et al* 2007 *Nucl. Fusion* 47 S1  
 [2] C. Giroud, et al, IAEA, 2021  
 [3] C. Giroud, et al, submitted to *Nucl. Fusion* 2024  
 [4] E. Kaveeva, et al, *Nucl. Materials and Energy*, 2021

The injection of neon for heat load control has an impact on the plasma profile and in particular decrease the pedestal density for all current in D and D-T. An example is shown in figure 7 comparing plasma profiles from unseeded to seeded plasmas with increased neon content, one can observe that the overall temperature profile is enhanced by seeding while the density profile is lower with increased neon seeding rate. However, because the temperature gain is higher than the density loss the pressure profile is also enhanced with neon seeding within this integrated scenario regime. It should be noted

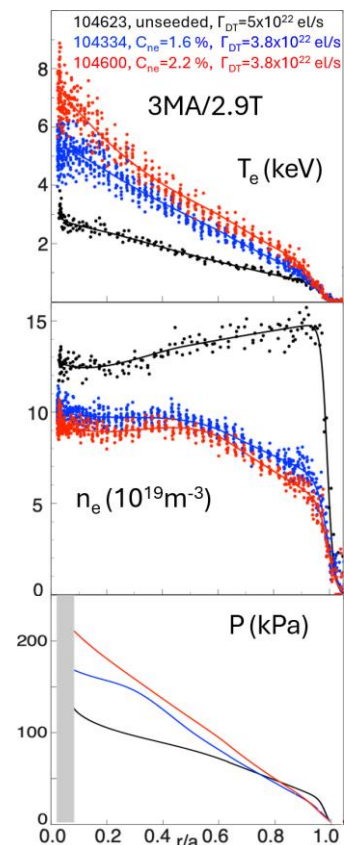


Figure 7 – Temperature, density, and pressure profiles for different neon levels.

[5] V. Rozhansky *et al* 2021 *Nucl. Fusion* 61 126073  
 [6] R.A. Pitts, et al, *Nucl. Materials and Energy*, 2019  
 [7] <https://www.youtube.com/watch?v=3ZyATi24BdU>  
 [8] J. Hobirk *et al* 2023 *Nucl. Fusion* 63 112001